Sensors and Materials, Vol. 30, No. 12 (2018) 2989–2998
MYU Tokyo

S & M 1735

Fabrication of Graphene Microroll Aptasensor

Yuko Ueno,[1*] Tetsuhiko Teshima,[1] Calum S. Henderson,[1,2] and Hiroshi Nakashima[1]

[1]NTT Basic Research Laboratories, NTT Corporation,
3-1 Morinosato Wakamiya, Atsugi, Kanagawa 243-0198, Japan
[2]School of Chemistry, University of Edinburgh, David Brewster Road, Edinburgh EH9 3FJ, UK

(Received July 31, 2018; accepted September 12, 2018)

Keywords: graphene, aptamer, biosensor, self-folding, microdevice

We have successfully created a graphene microroll aptasensor (GMA) through the self-folding of bilayer thin films. The inner surface of the GMA consists of a functionalized graphene surface, which works as a fluorescence aptamer-based biosensor. This is achieved by combining previously reported two-dimensional (2D) graphene aptasensor technology, a novel self-folding process for flexible, multilayered polymeric films. The aptasensing portion is composed of a graphene surface, which is functionalized with a pyrene–aptamer–dye probe. The three components of the probe work as linkers to the graphene surface, a protein recognition part, and a fluorescence detection tag, respectively. In this paper, we discuss the specialized fabrication process required to produce the GMA. By confirming the diffusion of target molecules through the hollow space of the GMA, we also show the ability of this device to detect concentration changes in real time.

1. Introduction

Cells, which are constituent units of organisms, continuously synthesize proteins, nucleic acids, and lipids in order to maintain their forms, proliferate, and communicate. It is important to investigate how the synthesized metabolites are consumed or released by the cells in order to understand the real-time activity and compare various cell types. In recent years, it has become possible to use microfabrication techniques for the manipulation of individual cells, enabling the investigation of the expression level and localization of excreted substances, while controlling the behavior and morphology of target cells.[1–3] However, it is still difficult to perform the quantitative analysis of the substances secreted and released from the cells across the cell membrane at the single-cell level because of their diffusive nature after secretion. If an accurate quantitative analysis of extracellular secreted substances becomes possible, it will lead to a better understanding of cellular responses to changes in their external environment. A microdroplet has been used to measure cell metabolites by encapsulating single cells and their secreted metabolites within its closed space.[4] However, an integrated sensor that can detect extracellular secreted substances quantitatively in real time has not been reported yet.

*Corresponding author: e-mail: ueno.yuko@lab.ntt.co.jp
https://doi.org/10.18494/SAM.2018.2069

ISSN 0914-4935
https://myukk.org/

As regards a real time and label-free biosensor, we have developed an aptasensor that works on a graphene surface for the detection of biologically important proteins such as cancer markers.[5,6] In our system, the graphene surface is functionalized with a pyrene–aptamer–dye probe. The three components of the probe work as linkers to the graphene surface, a protein recognition part, and a fluorescence detection tag, respectively. Here, graphene behaves simultaneously as both an efficient acceptor for fluorescence resonance energy transfer (FRET) and a strong adsorbate for aptamers.[7] The graphene aptasensor detection mechanism is as follows. In the initial stage, the dye-conjugated aptamer is adsorbed on the graphene surface via π–π interactions, and thus the dye is located close to the graphene surface. Here, the fluorescence of the dye is well quenched by the graphene and is barely visible [Fig. 1(a, left)]. If the target of the aptamer is present in the system, the aptamer forms a complex with the target and leaves the graphene surface. At the same time, the dye molecule also leaves the graphene surface and the dye recovers its fluorescence [Fig. 1(a, right)]. The target can be detected in real time simply by adding a sample with a volume smaller than 1 μL to a sensor chip [Fig. 1(b)]. If we can build our two-dimensional (2D) sensor in a three-dimensional (3D) structure that can encapsulate living cells, we can create an integrated sensor capable of real-time monitoring of extracellular secreted substances [Fig. 1(c)].

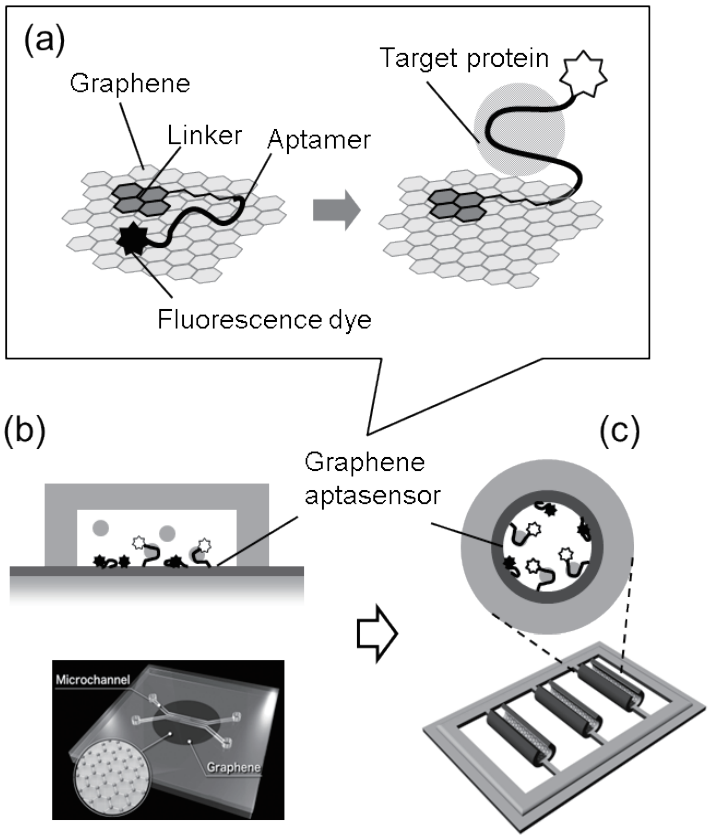

Fig. 1. (a) Design of protein detection system of graphene aptasensor, (b) conceptual illustration of our previous on-chip graphene aptasensor using 2D plane, and (c) GMA.

We have also reported that multilayered polymeric films with heterogeneous mechanical properties can form self-folded microrolls.[8,9] Through integration with a noncytotoxic batch release of a hydrogel-based sacrificial layer, the films autonomously fold into cylindrical shapes on the basis of differential strain gradients that depend on the film thickness. Various 3D cell-laden microstructures form from 2D geometrical micropatterns, enabling the embedded cells to migrate and connect with each other. Within a microcavity, they tend to form the desired 3D architectures and synchronize their behavior. By integrating graphene aptasensors with this microroll technology, we can easily perform highly sensitive and real-time measurement of a target substance secreted from a live cell culture within a micrometer-sized 3D space. Moreover, inside the microroll, molecules diffuse at a lower rate and are thus easily trapped within the sensing space, making their detection much easier.

In this study, we successfully combined the graphene-based aptasensor and self-folded microrolls to create a fluorescence graphene aptasensor formed on the inner wall of a hollow 3D structure [Fig. 1(c)]. We demonstrated a detailed fabrication procedure for a graphene microroll aptasensor (GMA) that allows for nontoxic cell encapsulation and monitoring.

2. Materials and Methods

2.1 Materials

A CVD-grown single-layer graphene on Cu foil was purchased from Graphene Platform Corporation (Tokyo, Japan). The synthetic oligonucleotide with a prostate-specific antigen (PSA) aptamer sequence and an extra-10-thymine sequence with an amino group and a red-fluorescent TAMRA [λ_{max}(abs)/λ_{max}(em) = 555 nm/580 nm] at the 5′ and 3′ termini, namely, 5′NH_2-TTTAATTAAAGCTCTCCATCAAATAGCTTTTTTTTTT-TAMRA′ (2), was purchased from Sigma Genosys. Dichloro-di(*p*-xylylene) (parylene, DPX-C) powder was purchased from Speedline Technology, USA. Aqueous silk fibroin solution was extracted from the cocoons of *Bombyx mori* (*B. mori*) silkworm. 1-Pyrenebutanoic acid-succinimidyl ester (Invitrogen), *N*,*N*-dimethylformamide (DMF, Kanto Chemical Co., Inc.), phosphate buffer (pH = 7.4, Nacalai Tesque), ethylene-diaminetetraacetic acid (EDTA, Nacalai Tesque), sodium alginate (Sigma), calcein (Dojindo Molecular Technologies, Inc.), and 45% of Fe(III)Cl_3 solution (Aldrich) were used as received. Deionized (DI) water (Millipore, >18 MΩ·cm) was used throughout the work.

2.2 Measurements

An Olympus FV1200 inverted confocal laser scanning microscopy (LSM) system was used to obtain fluorescence and differential interference images. We used a 565 nm high-pass filter for the fluorescence observations of TAMRA with a 543 nm laser light source through a glass plate with an objective lens (UPlan Apo 10× LSM).

We measured the Raman spectra employing a Raman microprobe system (inVia Reflex/StreamLine microRaman spectrometer, Renishaw) using a CCD detector. The excitation light sources used were the 532 nm lines of a laser-diode continuous-wave laser. The maximum

laser power focused on the sample with an objective lens (×100, NA 0.85) was about 35 mW for all the measurements. The spot size and focal depth on the sample were about 1 and <10 μm, respectively. The scattered light was collected using a 180° backscattering geometry, and the grating in the polychromator was 1800 line/mm.

2.3 Fabrication of GMA

The beginning part of the fabrication process of the GMA was similar to that we previously reported to form a self-folding microroll.[8,9] First, sodium alginate was coated on SiO_2 substrates and the coated substrates were then immersed in calcium chloride to hydrogelate alginate with calcium ions. Next, the aqueous silk fibroin was coated and hydrogelated by immersing in methanol, and then the chemical deposition of the parylene layer was performed. Subsequently, a single-layer graphene was transferred on the parylene layer in the same way as we previously reported to prepare a graphene aptasensor.[6] Next, a micropattern was formed on the plates by photolithography using oxygen plasma to etch the patterns into the multilayered films of alginate hydrogel, silk fibroin, parylene, and graphene. The photoresist mask was then removed using acetone. Finally, the graphene surface was functionalized with an aptamer to realize the GMA, with the method described in detail in the following section.

Figure 2 shows how to form the GMA via self-folding after fabricating the multilayered laminar films. We first soaked the patterned SiO_2 substrates in DI water and then EDTA was added to dissolve the Ca alginate sacrificial layer and trigger the folding from the rectangular pattern to a hollow cylinder [Fig. 2(a)]. Upon the addition of EDTA, the upper layers, multilayered laminar films consisting of silk fibroin, parylene, and aptamer-functionalized graphene, were released from the substrate [Fig. 2(b)]. The different strain gradients between

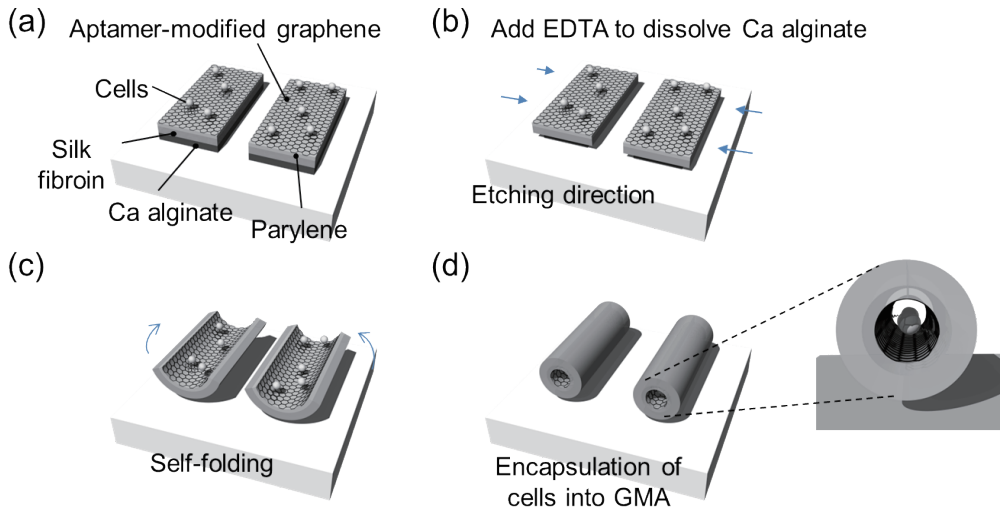

Fig. 2. Procedure for forming cell-encapsulated GMA after the patterned multilayered laminar films were prepared.

the layers act as the driving force behind the 3D transformation to microrolls [Fig. 2(c)]. As a result, hollow cylinders with aptamer-functionalized graphene on the inner surface, namely, the GMA, were produced. Note that the formation of microroll inhibits any cytotoxic processes. Thus, if we put living cells prior to the self-folding process, microrolls can be used as containers to encapsulate living cells [Fig. 2(d)].

3. Results and Discussion

3.1 Protocol for functionalizing graphene surface with aptamer

As we described in Sect. 2.3, we functionalized the graphene surface with an aptamer after we prepared the patterned multilayered laminar films. First, we employed the same protocol as that we used for the 2D aptasensor as follows. The graphene surface located at the top of the patterned multilayered laminar films was covered with a drop of 5 mM DMF solution of the linker (1-pyrenebutanoic acid-succinimidyl ester) for 1 h, rinsed with DMF, and then dried in a nitrogen stream. Then, 100 μM aptamer solution in phosphate buffer (10 mM, pH 7.4) was poured on the graphene surface and allowed to remain for 1 h. The amine group at the 3'-terminus of the aptamer was bonded to the pyrene linker by a dehydration reaction and thus the aptamer was immobilized on the graphene surface. It was at this point that we encountered some problems. The patterned multilayered laminar films were released from the glass substrate within 2–3 min after immersion in the aptamer solution, and thus we were unable to continue. As the phosphate buffer contains monovalent cations such as Na^+ and K^+, the dissolution of the Ca altginate sacrificial layer occurred upon the addition of the buffer. Figures 3(a)–3(c) show the changes in the patterned multilayered laminar films after immersion in 10 mM phosphate buffer (pH 7.4) for 0, 120, and 500 s, respectively. As we described, some parts of the patterned multilayered laminar films were released from the glass substrate at 120 s and the pattern was almost entirely peeled off at 500 s.

Therefore, we modified this step by using the 50 μM aptamer solution dissolved in a 1:1 mixture of 10 mM phosphate buffer solution (pH 7.4) and DMF, instead of using the 100 μM aptamer solution in phosphate buffer (10 mM, pH 7.4). We thought that mixing a certain concentration of organic solvent may suppress the dissolution of the Ca alginate sacrificial layer. We found that the patterned multilayered laminar films immersed in the solution for 1 h showed no serious damage even after rinsing with DMF and drying in a nitrogen stream. Figure 3(d) shows the patterned multilayered laminar films formed on the same substrate as that shown in Figs. 3(a)–3(c), 3000 s after adding the same amount of DMF to 10 mM phosphate buffer in order to immerse the films in the 1:1 mixture of 10 mM phosphate buffer solution (pH 7.4) and DMF. The patterns were completely stable in this environment. We then rinsed the substrate with DMF, dried in a nitrogen stream, and then immersed in ~5 mM EDTA solution. After roughly 150 s, the formation of microrolls was clearly observed. The results indicate that the 1:1 mixture of 10 mM phosphate buffer solution (pH 7.4) and DMF is a practical solvent to be used in the aptamer functionalization step in GMA fabrication.

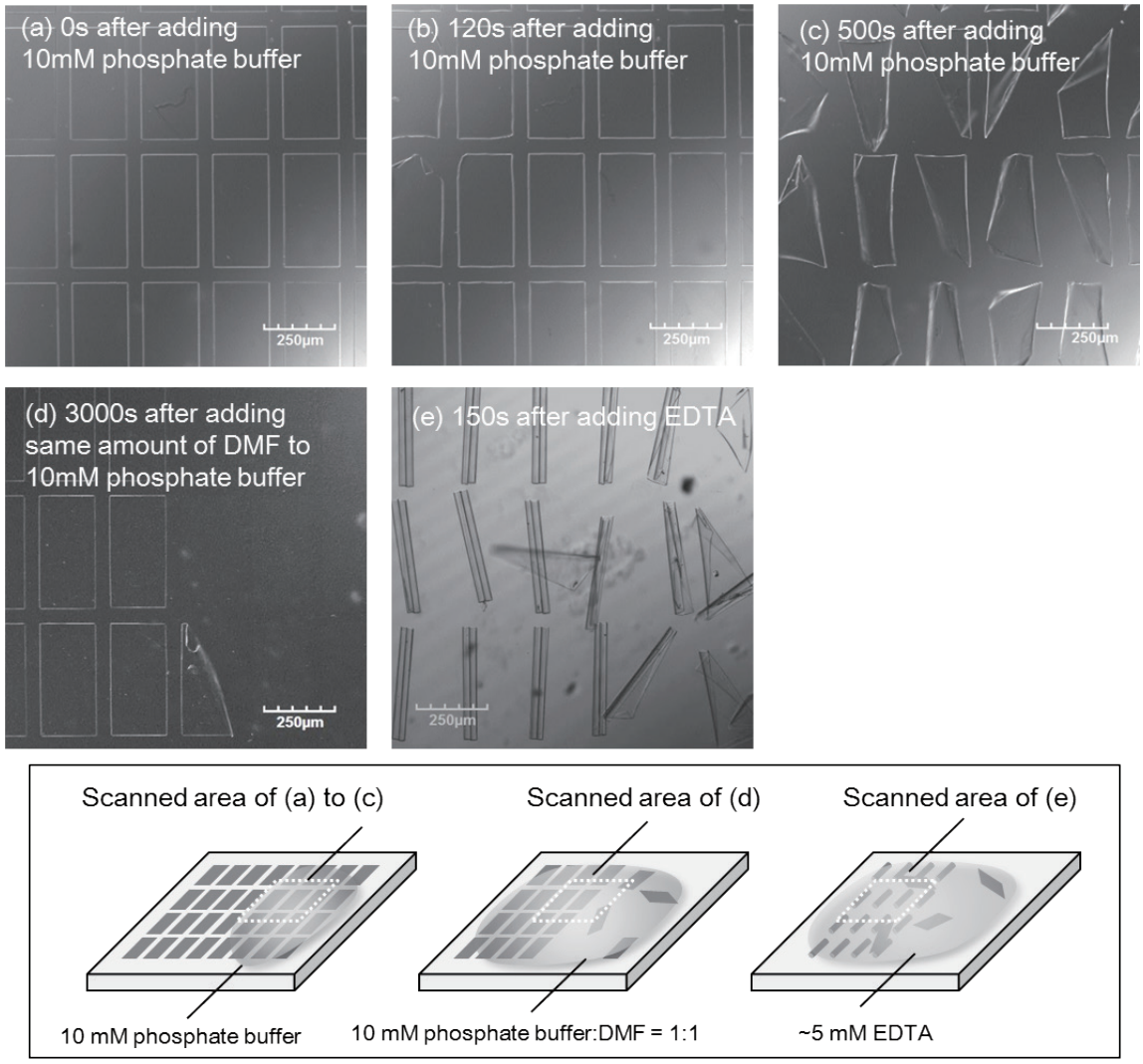

Fig. 3. Optical images of patterned multilayered laminar films after immersion in 10 mM phosphate buffer (pH 7.4) for (a) 0, (b) 120, (c) 500, and (d) 3000 s after adding same amount of DMF to 10 mM phosphate buffer in order to immerse the films in 1:1 mixture of 10 mM phosphate buffer solution (pH 7.4) and DMF, and (e) 150 s after immersion in ~5 mM EDTA solution after step (d), rinsing the substrate with DMF and drying in a nitrogen stream. The bottom images illustrate the scanned area of each image.

3.2 Self-folding of GMA

Figure 4(b) shows the observed results of the self-folding of the GMA patterned as an 800×300 μm^2 rectangle. We first soak the patterned SiO_2 substrates in DI water. After adding EDTA, the dissolution of the Ca alginate sacrificial layer caused the release of multilayered laminar films consisting of silk fibroin (thickness: ~180 nm), parylene (thickness: ~150 nm), and aptamer-functionalized graphene from the substrate, and the successful formation of tubular GMA structures through self-folding was observed within 160 s.

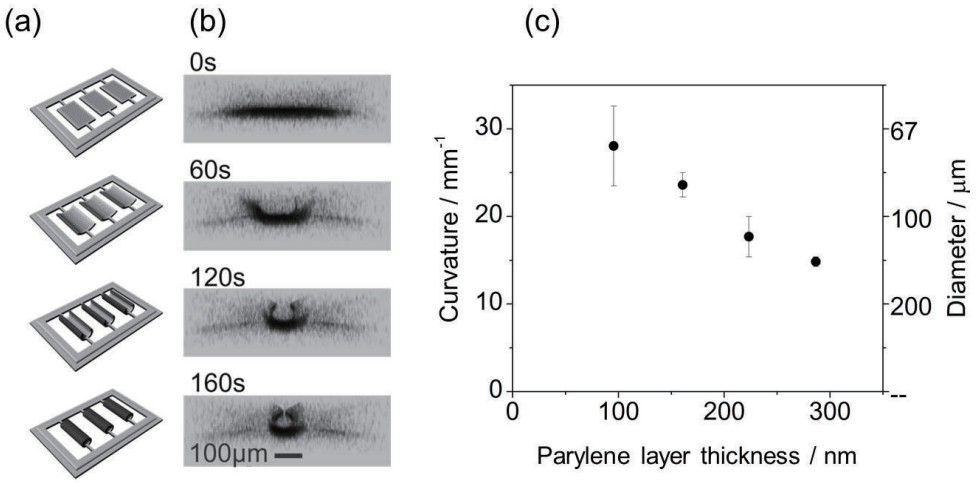

Fig. 4. (a) Observation of self-folding of GMA. Conceptual illustration of overall view, (b) the side views recorded before (0 s) and 60, 120, and 160 s after removing the sacrifice layer, and (c) dependence of curvature/diameter of GMA dependence on the thickness of the parylene layer.

Since the underlying mechanism of self-folding is the stiffness mismatch in the bilayer as we reported previously, the curvature of a microroll can be estimated by theoretical calculation.[10,11] Figure 4(c) shows the curvature/diameter dependence on the thickness of the parylene layer. Here, we set the thickness of silk fibroin to be constant at ~180 nm and varied the thickness of parylene from 100 to 300 nm. We found that the diameter of the GMA increased with the parylene layer thickness; thus, we can control the size of the GMA by choosing the desired thickness of the parylene layer.

Next, we studied whether the graphene layer is damaged during the entire process. We measured the Raman spectra of the GMA before and after self-folding (Fig. 5). The characteristic peaks of G and 2D bands of graphene are present both before and after folding at ~1580 and ~2680 cm^{-1}, respectively, indicating that the graphene monolayer was undamaged by the folding process. Thus, we expect that the sensing performance of the GMA will be similar to that of the previous 2D graphene aptasensor.

3.3 Diffusion of molecules in GMA

As regards the application of GMA, we expect that the highly sensitive quantitative detection of molecules will be possible by decreasing the rate of molecular diffusion inside a microroll to the bulk solution. Preventing the dilution of biomarker proteins secreted from the bulk solution works as a merit because keeping a high target molecule concentration for a long time makes detection much easier. In order to study the molecular diffusion rate, we immersed the GMA in fluorescent calcein dye solution and then washed with water. We monitored the change in fluorescence intensity at 10 s intervals at the center and entrance of the GMA and determined the time to reach the same levels as those outside the GMA (Fig. 6). At the center of the GMA,

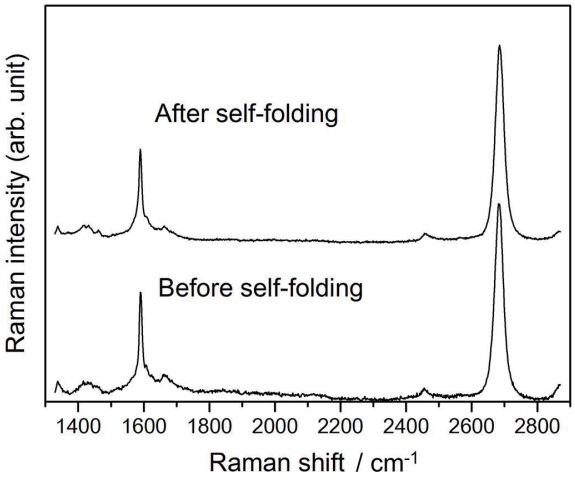

Fig. 5. Raman spectra of GMA obtained before (lower) and after (upper) self-folding.

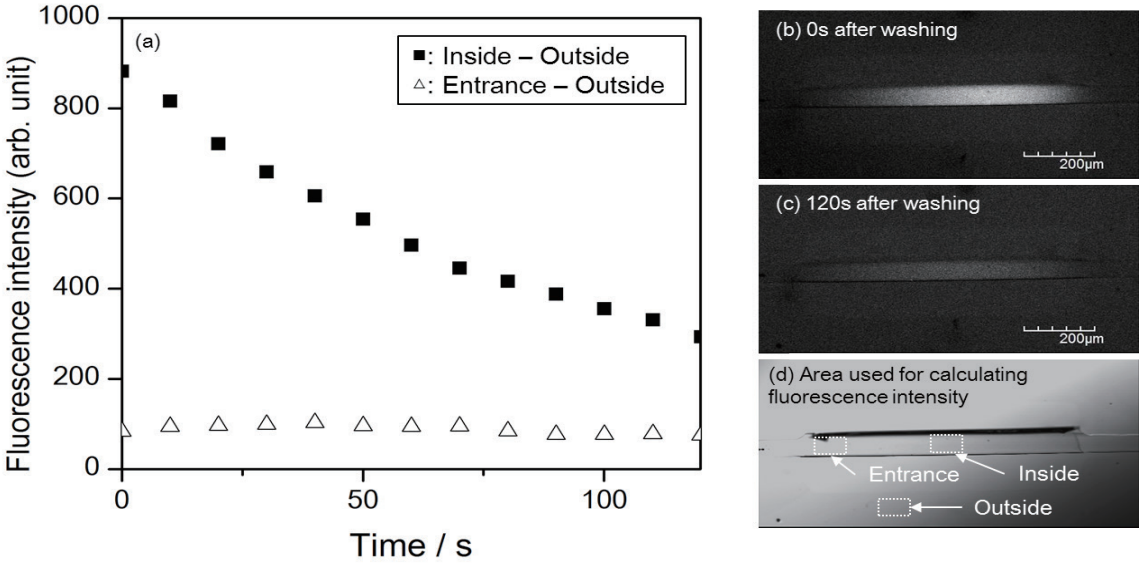

Fig. 6. (a) Changes in the fluorescence intensity of ■ (inside–outside) and △ (entrance–outside) of GMA against time. Fluorescence images of GMA obtained (b) 0 and (c) 120 s after washing calcein dye solution, and (d) the optical image showing the area used for calculating fluorescence intensity.

the fluorescence intensity was more than 8 times higher than that at the entrance just after washing and continued to be more than 3 times higher even 120 s after washing. The results indicate that proteins, which are molecules much larger than calcein, can have a lower diffusion rate and thus can easily be trapped within the GMA for a long time. Therefore, the GMA will be a promising tool for making the detection of target molecules much easier than that in the case of conventional 2D biosensors.

4. Conclusions

We created a GMA whose inner wall surface consists of a functionalized single graphene. The graphene layer in GMA works as a fluorescence aptamer-based biosensor, achieved by combining the previously reported 2D graphene aptasensor and self-folded microrolls that can be used for nontoxic cell encapsulation. We found that the 1:1 mixture of 10 mM phosphate buffer solution (pH 7.4) and DMF is a practical solvent to be used in the aptamer functionalization step in the fabrication of the GMA. The Raman measurement reveals that the graphene monolayer is undamaged during the self-folding process and thus we expect that the sensing performance of the GMA will be similar to that of the previous 2D graphene aptasensor. We also found that the diffusion of calcein dye was much slower from inside the GMA to the bulk solution. Thus, molecules larger than calcein can have a lower diffusion rate and can easily be trapped within the GMA for a long time. We conclude that the GMA will be a promising tool much easier detection of target molecules than in the case of conventional 2D biosensors.

Acknowledgments

This work was supported by JSPS KAKENHI Grant Number JP17H02759.

References

1 T. Teshima, H. Onoe, H. Aonuma, K. Kuribayashi-Shigetomi, K. Kamiya, T. Tonooka, H. Kanuka, and S. Takeuchi: Adv. Mater. **26** (2014) 2850. https://doi.org/10.1002/adma.201305494
2 T. Teshima, H. Nakashima, N. Kasai, S. Sasaki, A. Tanaka, S. Tsukada, and K. Sumitomo: Adv. Funct. Mater. **26** (2016) 8185. https://doi.org/10.1002/adfm.201603302
3 T. Teshima, H. Onoe, S. Tottori, H. Aonuma, T. Mizutani, K. Kamiya, H. Ishihara, H. Kanuka, and S. Takeuchi: Small **12** (2016). https://doi.org/10.1002/smll.201600339
4 B. Kintses, C. Hein, M. F. Mohamed, M. Fischlechner, F. Courtois, C. Lainé, and F. Hollfelder: Chem. Biol. **19** (2012) 1001. http://dx.doi.org/10.1016/j.chembiol.2012.06.009
5 Y. Ueno, K. Furukawa, K. Matsuo, S. Inoue, K. Hayashi, and H. Hibino: Anal. Chim. Acta **866** (2015) 1. https://doi.org/10.1016/j.aca.2014.10.047
6 K. Furukawa, Y. Ueno, M. Takamura, and H. Hibino: ACS Sens. **1** (2016) 710. https://doi.org/10.1021/acssensors.6b00191
7 L. Gao, C. Lian, Y. Zhou, L. Yan, Q. Li, C. Zhang, L. Chen, and K. Chen: Biosens. Bioelectron. **60** (2014) 22. https://doi.org/10.1016/j.bios.2014.03.039
8 T. F. Teshima, H. Nakashima, Y. Ueno, S. Sasaki, C. S. Henderson, and S. Tsukada: Sci. Rep. **7** (2017) 17376. https://doi.org/10.1038/s41598-017-17403-0
9 T. F. Teshima, C. S. Henderson, M. Takamura, Y. Ogawa, S. Wang, Y. kashimura, S. Sasaki, T. Goto, H. Nakashima, and Y. Ueno: Nano Lett. (accepted). https://doi.org/10.1021/acs.nanolett.8b04279
10 S. Tinoshenko: J. Opt. Soc. Am. **11** (1925) 233. https://doi.org/10.1364/JOSA.11.000233
11 J. Zang and F. Liua: Appl. Phys. Lett. **92** (2008) 021905. https://doi.org/10.1063/1.2828043

About the Authors

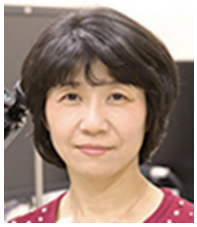

Yuko Ueno received her B.S., M.S., and Ph.D. in chemistry from the University of Tokyo in 1995, 1997, and 2002, respectively. She joined NTT Integrated Information & Energy Systems Laboratories in 1997. She was a postdoctoral fellow at the University of California at Berkeley and at Lawrence Berkeley National Laboratory, Berkeley, CA, USA, from 2004 to 2005. She is a member of the Japan Society of Analytical Chemistry, The Chemical Society of Japan, The Spectroscopical Society of Japan, The Japan Society of Applied Physics, The Japan Society of Vacuum and Surface Science, Society for Chemistry and Micro-Nano Systems, and The Institute of Electronics, Information and Communication Engineers.
(ueno.yuko@lab.ntt.co.jp)

Tetsuhiko Teshima received his B.E., M.E., and Ph.D. degrees from the School of Agriculture, Arts and Science, and Information Science and Technology at the University of Tokyo, Japan in 2009, 2011, and 2014, respectively. From 2011 to 2014, he was a research fellow of Japan Society Promotion and Science (JSPS). He joined NTT Basic Research Laboratories in 2014 and is currently working on the silk fibroin-based biocompatible interface with skin and in vivo tissues to monitor vital data. He is a member of the Materials Research Society (MRS) of USA and the Japan Society of Applied Physics. (teshima.tetsuhiko@lab.ntt.co.jp)

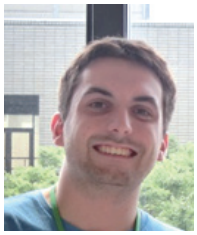

Calum S. Henderson has completed a Masters degree in Chemical Physics at the School of Chemistry, the University of Edinburgh, Scotland. He joined NTT Basic Research Laboratories in 2017 in the industrial placement program. He will join the ISIS Neutron and Muon Source, England as a researcher in 2018. (s1306753@sms.ed.ac.uk)

Hiroshi Nakashima received his B.E., M.E., and Ph.D. degrees in applied chemistry from Waseda University, Tokyo, in 1995, 1997, and 2002, respectively. He joined NTT Basic Research Laboratories in 1997. Since then, he has been engaged in research on the synthesis and control of the optoelectrical properties of (semi)conductive polymers and nano-biomaterials. He is a member of the Chemical Society of Japan (and its Colloid and Surface Chemistry Division) and the Japan Society of Applied Physics (and its Molecular Electronics and Bioelectronics Division). (nakashima.hiroshi@lab.ntt.co.jp)